A new computational method for transient dynamics including the low- and the medium-frequency ranges

Pierre Ladevèze, Mathilde Chevreuil

A new computational method for transient dynamics including the low- and the medium-frequency ranges

Pierre Ladevèze* and Mathilde Chevreuil

LMT Cachan (ENS Cachan, CNRS, University Paris 6),

61 avenue du Président Wilson, 94235 Cachan CEDEX, France

This paper deals with a new computational method for transient dynamic analysis which enables one to cover both the low- and medium-frequency ranges. This is a frequency approach in which the low-frequency part is obtained through a classical technique while the medium-frequency part is handled through the Variational Theory of Complex Rays (VTCR) initially introduced for vibrations. Preliminary examples are shown.

KEY WORDS: Dynamics; frequency domain; medium frequencies; computation

1. INTRODUCTION

The design of industrial structures requires engineers to know their dynamic behavior. The response, especially during the transient stage, cannot be completely described using the current tools based on finite element techniques and explicit numerical schemes; indeed, the medium-frequency range is often ignored unless the calculation is carried out with a very refined spatial mesh and, consequently, a refined time discretization [1, 2]. This would mean a prohibitive computation time. Accounting for the medium-frequency content can be necessary because although the displacements over this frequency range are small, the velocity (and, therefore, the kinetic energy) can be significant. Transient dynamic analysis in this frequency range presents an important challenge. This work, which uses new computational strategies in dynamics, provides an answer to this challenge for the transient part of the solution. The problem is solved in the frequency domain. One needs to solve a forced vibration problem over a frequency range which includes the low- and medium-frequency ranges. The low-frequency range is solved conventionally while the medium-frequency range is handled using the Variational Theory of Complex Rays (VTCR). The final solution in the space-time domain is given by the inverse of the Fourier transform.

*Correspondence to: a

*Correspondence to: LMT Cachan, 61 avenue du Président Wilson, 94235 Cachan CEDEX, France.

†E-mail: pierre.ladeveze@lmt.ens-cachan.fr

The main problem resides in the resolution of the forced vibration problem over a wide frequency range. Today, the low-frequency range no longer poses any major difficulty, at least regarding modeling and calculation, even for complex structures. As for high frequencies, computational tools quite different from those used for low frequencies are available, in particular the SEA method in which the spatial aspects disappear almost entirely [3].
By contrast, the modeling and calculation of medium-frequency vibrations, on which this paper focuses, continue to cause some problems. The difficulty lies in the fact that the wavelengths of the phenomena being studied are very small compared to the characteristic dimensions of the structure. Consequently, if one were to extend the low-frequency methods disregarding the serious numerical difficulties Which would occur, the corresponding finite element calculation would still require an unreasonable number of degrees of freedom. This situation would be made even worse by the pollution error due to the extended range of calculated frequencies which would affect the accuracy of the finite element solution [4, 5]. Different remedies for that problem have been tried, such as enhanced finite elements [6, 7, 8], specific reduced bases [9, 10, 11] or a combination of a wave-based method with a Trefftz approach [12], but most of these techniques require very fine meshes. Difficulties are also experienced when one attempts, as in [13, 14, 15, 16], to extend the SEA method (which is appropriate for high frequencies) because most of these methods require additional information (e.g. coupling loss factors) and specific geometries.
The alternative approach we use here, called the "Variational Theory of Complex Rays", was first introduced in [17] for the calculation of medium-frequency vibrations. It shares similar features with [12]. This approach, whose main limitation is that the structure must lend itself to partitioning into homogeneous substructures, is defined as follows.
The first characteristic of this approach is the use of a new variational formulation of the problem being considered (i.e. forced vibrations at a given frequency) which enables one to use *a priori* independent approximations within each substructure. In other words, the transmission conditions on the displacements as well as the stresses at the interfaces between substructures do not need to be verified *a priori*, but are built in the variational formulation.
The second characteristic of the VTCR is the introduction within each substructure of two-scale approximations with a strong mechanical meaning: the solution is assumed to be well-described as the superposition of an infinite number of local vibration modes. These basic modes (which can be interior modes, boundary modes or corner modes) verify the law of dynamics. All wave directions are taken into account and the unknowns are discretized amplitudes with relatively large wavelengths.

Thus, the present approach to the calculation of the transient dynamic response consists in dividing the frequency range being studied into two parts: the low-frequency range, over which the frequency response function is obtained with a standard finite element technique, and the medium-frequency range, in which the suitable method to calculate the frequency response function is the VTCR [18]. To improve the efficiency of the calculation, it is advantageous to use the VTCR over a relatively wide frequency range in order to decrease the cpu time: we will describe a corresponding enhancement of the method. This paper recalls only the basic aspects of the Variational Theory of Complex Rays.

The central objective of the paper is to present our new frequency-domain analysis procedure for transient dynamics and to show its effectiveness: indeed, the proposed method enables one to take into account the medium-frequency content of the transient response of a structure subjected to a shock. These medium frequencies make up a significant portion of the kinetic energy of the system. The paper also aims to show that the large-frequency-range solution provided by the VTCR is necessary in order to carry out discrete Fourier transforms easily and with reasonable numerical effort. An example is

detailed at the end of the paper.

2. THE DYNAMIC REFERENCE PROBLEM

Let us consider, under the assumptions of small perturbations, the dynamic equilibrium of a structure defined in the space domain Ω, and let $\partial\Omega$ be the boundary of Ω. At each time t of the interval $[0,T]$ being studied, this structure is subjected to the following actions:

- a displacement field $\underline{U_d}$ on a portion $\partial_1\Omega$ of boundary $\partial\Omega$,
- a force density $\underline{F_d}$ on the portion $\partial_2\Omega$ of $\partial\Omega$ which is the complementary part of $\partial_1\Omega$,
- a force density $\underline{f_d}$ on the whole domain Ω.

For every $\underline{M}$ belonging to Ω, the displacements are subjected to initial conditions at $t=0$:

$$\underline{U}_{|t=0} = \underline{U}_0 \tag{1}$$

$$\frac{\mathrm{d}\underline{U}}{\mathrm{d}t}_{|t=0} = \underline{\dot{U}}_0 \tag{2}$$

where $\underline{U}_0$ and $\underline{\dot{U}}_0$ are given.

Let us also define for the structure Ω the constitutive relation:

$$\boldsymbol{\sigma} = \mathbf{K}\boldsymbol{\varepsilon}(\underline{U}) + \eta\mathbf{K}\dot{\boldsymbol{\varepsilon}}(\underline{U})$$

where $\mathbf{K}$ is the Hooke's operator. In the present work, damping is introduced classically in terms of the frequency with $\eta > 0$, so the reference problem has a unique solution. More complex constitutive relations could also be taken into account.

The reference frame is assumed to be Galilean. The reference problem of the evolution of the structure during $[0,T]$ can be formulated as follows: Find $\underline{U}(\underline{M},t) \in \mathcal{U}^{[0,T]}$ and $\boldsymbol{\sigma}(\underline{M},t) \in \mathcal{S}^{[0,T]}$, with $\underline{M} \in \Omega$ and $t \in [0,T]$, which verify:

- the compatibility equations and the initial conditions:

$$\underline{U}_{\partial_1\Omega} = \underline{U_d}$$
$$\underline{U}_{|t=0} = \underline{U}_0 \qquad \frac{\mathrm{d}\underline{U}}{\mathrm{d}t}_{|t=0} = \underline{\dot{U}}_0 \tag{3}$$

- the dynamic equilibrium equation:

$$\forall t \in]O,T[, \forall \underline{\dot{U}^*} \in \mathcal{U}_0$$
$$\int_\Omega \rho \frac{\mathrm{d}^2\underline{U}}{\mathrm{d}t^2}.\underline{\dot{U}^*}\,\mathrm{d}\Omega = -\int_\Omega \mathrm{Tr}[\boldsymbol{\sigma}\boldsymbol{\varepsilon}(\underline{\dot{U}^*})]\,\mathrm{d}\Omega + \int_\Omega \underline{f_d}.\underline{\dot{U}^*}\,\mathrm{d}\Omega + \int_{\partial_2\Omega} \underline{F_d}.\underline{\dot{U}^*}\,\mathrm{d}S \tag{4}$$

- the constitutive relation:

$$\boldsymbol{\sigma} = \mathbf{K}\boldsymbol{\varepsilon}(\underline{U}) + \eta\mathbf{K}\dot{\boldsymbol{\varepsilon}}(\underline{U}) \tag{5}$$

$\mathcal{U}_0$ is the subspace of $\mathcal{U}^{[0,T]}$ associated with a zero value of $\underline{U_d}$ on boundary $\partial_1\Omega$.

3. FREQUENCY ANALYSIS OF THE REFERENCE PROBLEM

3.1. Frequency formulation of the problem

Let us rewrite the transient dynamic problem as a global variational problem over the frequency-space domain. Thus, the Fourier transform is applied to all time-dependent quantities, yielding frequency-dependent functions:

$$\hat{f}(\omega) = \int_{-\infty}^{+\infty} f(t)\, \mathrm{e}^{-i\omega t}\, \mathrm{d}t \tag{6}$$

Thus, the reference problem can be reformulated as follows: Find $(\underline{\hat{U}}(\underline{M},\omega), \hat{\boldsymbol{\sigma}}(\underline{M},\omega))$, with $\underline{M} \in \Omega$ and $\omega \in \mathbb{R}$, which verify:

- the compatibility equations:

$$\begin{aligned} \underline{\hat{U}}_{\partial_1\Omega} &= \underline{\hat{U}}_d \\ \underline{\hat{\dot{U}}} &= i\omega\underline{\hat{U}} \end{aligned} \tag{7}$$

- the dynamic equilibrium equation:

$$\begin{aligned} &\forall \omega \in \mathbb{R}, \forall \underline{\hat{U}}^* \in \mathcal{U}_0 \\ &\int_\Omega -\rho\omega^2 \underline{\hat{U}}.\underline{\hat{U}}^*\, \mathrm{d}\Omega = -\int_\Omega \mathrm{Tr}[\hat{\boldsymbol{\sigma}}\boldsymbol{\varepsilon}(\underline{\hat{U}}^*)]\, \mathrm{d}\Omega + \int_\Omega \underline{\hat{f}}_d.\underline{\hat{U}}^*\, \mathrm{d}\Omega + \int_{\partial_2\Omega} \underline{\hat{F}}_d.\underline{\hat{U}}^*\, \mathrm{d}S \end{aligned} \tag{8}$$

- the constitutive relation:

$$\hat{\boldsymbol{\sigma}} = (1+i\eta)\mathbf{K}\boldsymbol{\varepsilon}(\underline{\hat{U}}) \tag{9}$$

Putting the accent on the displacement, the reference problem can be rewritten as: Find $\underline{\hat{U}}(\underline{M},\omega)$, with $\underline{M} \in \Omega$ and $\omega \in \mathbb{R}$, such that:

$$\underline{\hat{U}}_{\partial_1\Omega} = \underline{\hat{U}}_d$$

$$\begin{aligned} &\forall \omega \in \mathbb{R}, \forall \underline{\hat{U}}^* \in \mathcal{U}_0 \\ &\int_\Omega \left\{ -\rho\omega^2 \underline{\hat{U}}.\underline{\hat{U}}^* + (1+i\eta)\mathrm{Tr}[\mathbf{K}\boldsymbol{\varepsilon}(\underline{\hat{U}})\boldsymbol{\varepsilon}(\underline{\hat{U}}^*)] \right\} \mathrm{d}\Omega = \\ &\qquad \int_\Omega \underline{\hat{f}}_d.\underline{\hat{U}}^*\, \mathrm{d}\Omega + \int_{\partial_2\Omega} \underline{\hat{F}}_d.\underline{\hat{U}}^*\, \mathrm{d}S \end{aligned} \tag{10}$$

For a given ω, the previous problem is a forced vibration problem whose solution can easily be shown to be unique. Using the frequency approach, one needs to solve the forced vibration problem over a wide frequency range $[0, \omega'_c]$ which contains the low- and medium-frequency ranges; finally, one must calculate the frequency response function $\underline{\hat{h}}(\omega)$ of the system for $\omega \in [0, \omega'_c]$.

3.2. Principle of the new computational approach

The present approach considers a partition of the frequency range $[0, \omega'_c]$ being studied into two parts:

- a low-frequency part $[0, \omega_c]$,

- a medium-frequency part $[\omega_c, \omega'_c]$.

Outside of this frequency range, the kinetic and strain energies in the structure are assumed to be negligible.

For the low-frequency range $[0, \omega_c]$, the frequency response function is obtained using a finite element technique: it is advantageous to use a reduced basis constructed from the first vibration modes and completed with the static modes. With this very standard approach (see e.g. [**?**, 19]), the displacement can be written as:

$$\underline{\hat{U}}(\underline{M}, \omega) = \sum_{i=1}^{n} a_i(\omega)\underline{\varphi}_i(\underline{M}) + \sum_{j=1}^{m} b_j(\omega)\underline{\varphi'}_j(\underline{M}) \tag{11}$$

where $\underline{\varphi}_i(\underline{M})$ are the eigenmodes of the structure and $\underline{\varphi'}_j(\underline{M})$ are the static modes. The basis contains at least all the eigenvectors $\underline{\varphi}_i(\underline{M})$ such that $\omega_i \leq 2\,\omega_c$. The $\underline{\varphi}_i(\underline{M}), i \in \{1,2,...,n\}$ and $\underline{\varphi'}_j(\underline{M}), j \in \{1,2,...,m\}$ are constructed in such a way that they are orthogonal with respect to the kinetic energy.

The Variational Theory of Complex Rays (VTCR), which will be presented in Section 4, is a suitable computational method for the medium-frequency range $[\omega_c, \omega'_c]$.

For $\omega^- \leq 0$, the frequency response is the conjugate of the response with respect to the excitation's frequency $\omega^+ = -\omega^-$.

3.3. Back to the time response

After the frequency response functions of the points of interest in the structure have been calculated over $[0, \omega'_c]$, the time response is restored using the inverse Fourier transform:

$$f(t)_{t\geq 0} = \frac{1}{2\pi}\int_{-\infty}^{+\infty} \hat{f}(\omega)\,\mathrm{e}^{i\omega t}\,\mathrm{d}\,\omega \tag{12}$$

4. OUTLINE OF THE VTCR FOR THE RESOLUTION OF THE FORCED VIBRATION PROBLEM FOR THE MEDIUM-FREQUENCY PART

Only the basic aspects are given here. More details can be found in [20, 21, 22].

4.1. The reference problem

In order to simplify the presentation, we present the problem for an assembly of two substructures, but this formulation can be easily generalized to an assembly of n substructures. Given two substructures S and S', let ∂S and $\partial S'$ be the boundaries of S and S' respectively. We are studying the harmonic vibration of these two structures at a fixed frequency ω. All quantities can be defined in the complex domain: an amplitude $Q(\underline{M})$ is associated with $Q(\underline{M})\,\mathrm{e}^{i\omega t}$.

The excitations applied to S and shown in Figure 1 are:

- a displacement field $\underline{U}_d$ on a portion $\partial_U S$ of the boundary ∂S,
- a force density $\underline{F}_d$ on a portion $\partial_F S$ of ∂S,
- a force density $\underline{f}_d$ on the whole domain S,

where $\underline{U}_d$, $\underline{F}_d$, $\underline{f}_d$ are the amplitudes of the quantities defined in the complex domain.
Similar quantities are defined for S'.

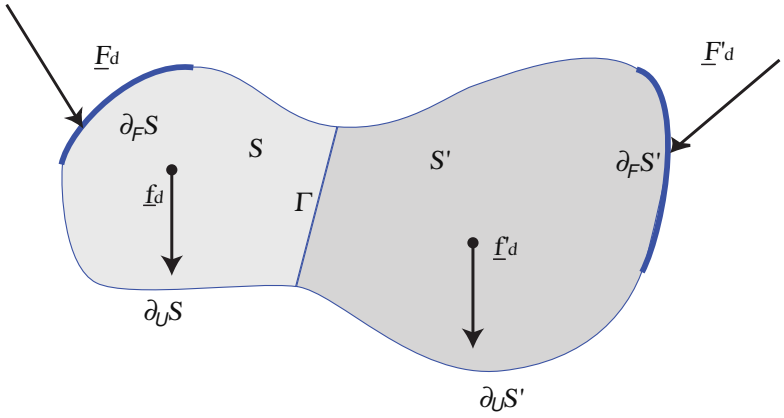

Figure 1. The reference problem

Let us define for structure S the displacement-stress pair $s = (\underline{U}, \boldsymbol{\sigma})$ and the corresponding space $\mathcal{S}_{ad}$ such that:

$$\begin{aligned}
&\underline{U} \in \mathbf{U} && \text{(finite-energy displacement set } [H^1(S)]^3) \\
&\boldsymbol{\sigma} \in \mathbf{S} && \text{(finite-energy stress set } [L^2(S)]^3) \\
&\underline{\Gamma} = \underline{div}\boldsymbol{\sigma} + \underline{f}_d && \text{on } S \\
&\boldsymbol{\sigma} = (1 + i\eta)\mathbf{K}\varepsilon(\underline{U}) && \text{on } S \\
&\underline{\Gamma} = -\omega^2 \rho \underline{U} && \text{on } S
\end{aligned} \tag{13}$$

where $\mathbf{K}$ is the Hooke's operator, ρ the mass density and η the damping coefficient (which depends on the frequency). The subspace of $\mathcal{S}_{ad}$ associated with a zero value of $\underline{f}_d$ is denoted $\mathcal{S}_{ad,0}$. Similarly, we introduce spaces $\mathcal{S}'_{ad}$ and $\mathcal{S}'_{ad,0}$.

The reference problem can be formulated as follows: Find $(\underline{U}(\underline{M}), \boldsymbol{\sigma}(\underline{M}), \underline{M} \in S)$ and $(\underline{U}'(\underline{M}), \boldsymbol{\sigma}'(\underline{M}), \underline{M} \in S')$ such that:

$$\begin{aligned}
&s = (\underline{U}, \boldsymbol{\sigma}) \in \mathcal{S}_{ad} && s' = (\underline{U}', \boldsymbol{\sigma}') \in \mathcal{S}'_{ad} \\
&\underline{U} = \underline{U}_d \text{ on } \partial_U S && \underline{U}' = \underline{U}'_d \text{ on } \partial_U S' \\
&\boldsymbol{\sigma}\underline{n} = \underline{F}_d \text{ on } \partial_F S && \boldsymbol{\sigma}'\underline{n}' = \underline{F}'_d \text{ on } \partial_F S' \\
&\underline{U} = \underline{U}' \text{ on } \Gamma \\
&\boldsymbol{\sigma}\underline{n} + \boldsymbol{\sigma}'\underline{n}' = \underline{0} \text{ on } \Gamma
\end{aligned} \tag{14}$$

4.2. The variational formulation associated with the VTCR

The VTCR is a global formulation of the boundary conditions (14) in terms of both displacements and forces. It is based on *a priori* independent approximations within the substructures: Find $s = (\underline{U}, \boldsymbol{\sigma}) \in$

$\mathcal{S}_{ad}$ and $s' = (\underline{U}', \boldsymbol{\sigma}') \in \mathcal{S}'_{ad}$ such that:

$$\begin{aligned}
\mathrm{Re}\Bigg\{ -i\omega \Bigg[& \int_{\partial_U S} \delta\boldsymbol{\sigma}\underline{n}(\underline{U}^* - \underline{U}_d^*)\,\mathrm{d}l + \int_{\partial_F S} (\boldsymbol{\sigma}\underline{n} - \underline{F}_d)\delta\underline{U}^*\,\mathrm{d}l + \\
& \int_{\partial_U S'} \delta\boldsymbol{\sigma}'\underline{n}'(\underline{U}'^* - \underline{U}'^*_d)\,\mathrm{d}l + \int_{\partial_F S'} (\boldsymbol{\sigma}'\underline{n}' - \underline{F}'_d)\delta\underline{U}'^*\,\mathrm{d}l + \\
\frac{1}{2}\int_\Gamma & (\delta\boldsymbol{\sigma}\underline{n} - \delta\boldsymbol{\sigma}'\underline{n}')(\underline{U}^* - \underline{U}'^*) + (\boldsymbol{\sigma}\underline{n} - \boldsymbol{\sigma}'\underline{n}')(\delta\underline{U}^* - \delta\underline{U}'^*)\,\mathrm{d}l \Bigg] \Bigg\} = 0 \\
& \forall (\delta\underline{U}, \delta\boldsymbol{\sigma}) \in \mathcal{S}_{ad,0} \quad \forall (\delta\underline{U}', \delta\boldsymbol{\sigma}') \in \mathcal{S}'_{ad,0}
\end{aligned} \tag{15}$$

where $\mathrm{Re}[A]$ designates the real part of a quantity A and A^* the conjugate of A. It is easy to prove that the variational form is equivalent to the reference problem, provided that:

- the reference problem has a solution,
- the Hooke's operator $\mathbf{K}$ is positive definite,
- the damping coefficients are such that $\eta, \eta' > 0$.

4.3. Approximate formulations

4.3.1. Principle All that is needed in order to derive an approximate formulation from the VTCR is the definition of subspaces $\mathcal{S}^h_{ad}$ and $\mathcal{S}^h_{ad,0}$ (resp. $\mathcal{S}'^h_{ad}$ and $\mathcal{S}'^h_{ad,0}$) from $\mathcal{S}_{ad}$ and $\mathcal{S}_{ad,0}$ (resp. $\mathcal{S}'_{ad}$ and $\mathcal{S}'_{ad,0}$) for each substructure. The approximate formulation can be expressed as: Find $s^h = (\underline{U}^h, \boldsymbol{\sigma}^h) \in \mathcal{S}^h_{ad}$ and $s'^h = (\underline{U}'^h, \boldsymbol{\sigma}'^h) \in \mathcal{S}'^h_{ad}$ such that:

$$\begin{aligned}
& \delta \quad E_D(\underline{U}^h) + E'_D(\underline{U}'^h) \quad + \left\langle \begin{bmatrix} s^h \\ s'^h \end{bmatrix}, \delta \begin{bmatrix} s^h \\ s'^h \end{bmatrix} \right\rangle = \quad L_D, \delta \begin{bmatrix} s^h \\ s'^h \end{bmatrix} \Bigg) \\
& \forall \delta s^h \in \mathcal{S}^h_{ad,0} \quad \forall \delta s'^h \in \mathcal{S}'^h_{ad,0}
\end{aligned} \tag{16}$$

where E_D is the dissipated power, L_D a linear form and $\langle .,. \rangle$ a bilinear form, defined on the boundary between the substructures, such that $\langle u, v \rangle = -\langle v, u \rangle^*$.

The VTCR uses two scales of approximation $(\underline{U}^h, \boldsymbol{\sigma}^h)$, each with a strong mechanical meaning, defined by identifying three zones: the interior zone, the edge zone and the corner zone. For example, in the neighborhood of a point $\underline{X}$ of the interior zone, the solution is assumed to be properly described locally as the superposition of an infinite number of local vibration modes which can be written in the following manner:

$$\begin{aligned}
\underline{U}^h(\underline{X}, \underline{Y}, \underline{P}) &= \underline{W}^h(\underline{X}, \underline{P})\, \mathrm{e}^{i\omega \underline{P}.\underline{Y}} \\
\boldsymbol{\sigma}^h(\underline{X}, \underline{Y}, \underline{P}) &= C^h(\underline{X}, \underline{P})\, \mathrm{e}^{i\omega \underline{P}.\underline{Y}}
\end{aligned} \tag{17}$$

where both $\underline{X}$ and $\underline{Y}$ represent the position vector, $\underline{X}$ being associated with slow variations and $\underline{Y}$ with rapid variations. More precisely, the terms related to the position vector $\underline{X}$ vary slowly when $\underline{X}$ moves along the structure, whereas the terms related to the position vector $\underline{Y}$ vary rapidly when $\underline{Y}$ moves along the structure. $\underline{P}$ is a vector characterizing the local vibration mode. In order for these local modes $(\underline{U}^h, \boldsymbol{\sigma}^h)$ to be admissible, they must be in $\mathcal{S}^h_{ad}$ and verify (13). Thus, we get some properties of $\underline{P}$.

For instance, let us consider the out-of-plane bending motions of thin, flat, homogeneous and isotropic plates. According to Kirchhoff's thin plate theory, the steady-state displacement u of the

plate's mid-surface in the direction perpendicular to the plate is governed by the dynamic equation:

$$\frac{Eh^3}{12(1-\nu^2)}(1+i\eta)\Delta\Delta u = \rho h\omega^2 u \text{ on } S \tag{18}$$

where Δ is the Laplacian operator, E the Young's modulus, h the plate's thickness, ν the Poisson's ratio, ρ the mass density, ω the frequency, and θ and η the damping factors. A complex ray for the interior modes is:

$$u_i^h(\underline{X},\underline{Y},\underline{P}) = w_i^h(\underline{X},\underline{P}) \, \mathrm{e}^{\left(\frac{\eta}{4}\sqrt{\omega}\underline{P}.\underline{X}\right) i\sqrt{\omega}\underline{P}.\underline{Y}} \tag{19}$$

This complex ray corresponds to a plane bending wave which propagates through the plate in the $\underline{P}$ direction. This ray is admissible only if:

$$\frac{Eh^3}{12(1-\nu^2)}(1+i\eta)\Delta\Delta w_i^h = \rho h\omega^2 w_i^h \text{ on } S \tag{20}$$

Therefore, the properties of $\underline{P}$ are:

$$(\underline{P}.\underline{P})^2 = r^4 \text{ with } r^4 = \frac{12\rho(1-\nu^2)}{Eh^2} \tag{21}$$

Equation (21) shows that $\underline{P}$ lies on a circle C defined by the material properties (see Figure 2). All directions of the plate can be taken into account by following this circular path. A similar approach can be used for the edge and corner zones. Examples of such modes are shown in Figure 3.

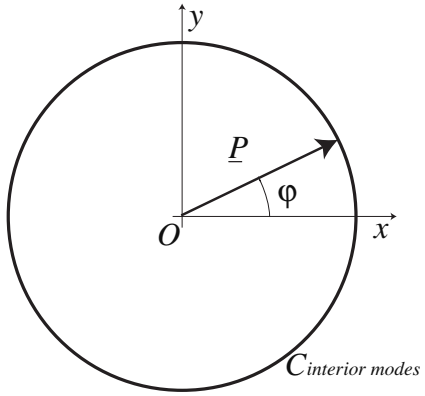

Figure 2. Admissible $\underline{P}$ for interior modes of an isotropic plate

4.3.2. The discretized problem The displacement of any point of the substructure is generated by a basis of admissible complex rays. The unknown is the generalized amplitude $w^h(\underline{X},\underline{P})$ of the basis (an n^{th}-order polynomial in $\underline{X}$ and a large-wavelength quantity). Accounting for all the directions φ in C leads to an integral over C. For the interior rays, this integral takes the form:

$$u^h(\underline{X},\underline{Y}) = \int_{\varphi\in[0;2\pi]} w^h(\underline{X},\underline{P}(\varphi)) \, \mathrm{e}^{\left(\frac{\eta}{4}\sqrt{\omega}\underline{P}(\varphi).\underline{X}\right) i\sqrt{\omega}\underline{P}(\varphi).\underline{Y}} \mathrm{d}\Gamma \tag{22}$$

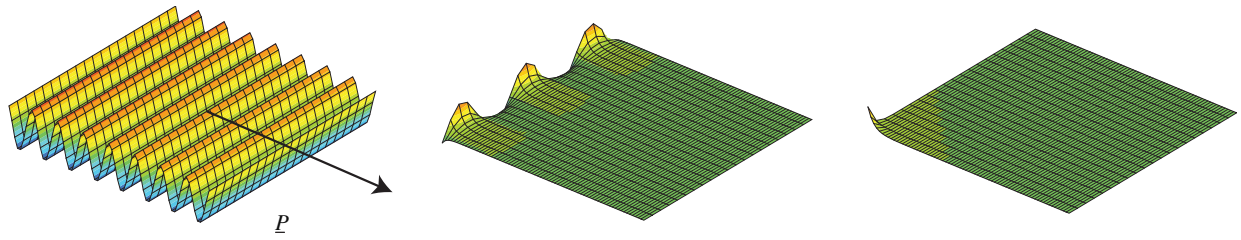

Figure 3. Interior, edge and corner modes for a homogeneous plate

In order to obtain a finite-dimension problem, this integral (22) can be discretized and one can consider the amplitude $w^h(\underline{X},\underline{P}(\varphi))$ to be constant in each angular sector: $w^h(\underline{X},\underline{P}(E_P))$ (Figure 4). The angular distributions of the plane waves for all points in the substructure are assumed to be well-described by this discontinuous angular distribution.

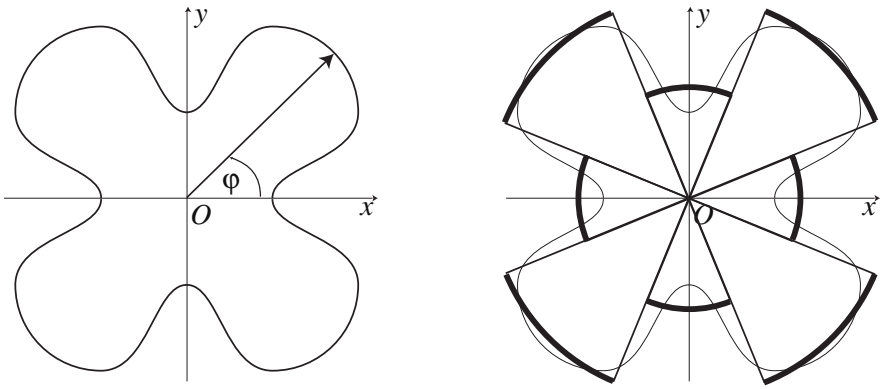

Figure 4. The discretized amplitudes

Once the discretization has been chosen for each plate, the VTCR leads to a system of linear equations in the complex domain:

$$\mathbf{K}^h \underline{U} = \underline{F}^h \tag{23}$$

where $\mathbf{K}^h = \mathbf{K}^h_s + \mathbf{Z}^h$ and $\underline{F}^h = \underline{L}^h_D$. $\mathbf{K}^h_s$ is the symmetric, positive definite damping matrix associated with E_D; $\mathbf{Z}^h$ is the matrix associated with the bilinear form $\langle .,. \rangle$ defined such that $\mathbf{Z}^{h,T^*} = -\mathbf{Z}^h$; $\underline{L}^h_D$ is the vector associated with the linear form L_D; $\underline{U}$ is the vector corresponding to the unknown amplitudes associated with the complex polynomial $w^h(\underline{X},E_P)$. As a consequence of the above properties, Equation (23) has a unique solution. However, although the invertibility of matrix $\mathbf{K}$ (and, therefore, the uniqueness of the solution) has been proven, care is needed in its numerical calculation because this theory could lead to a poorly conditioned matrix $\mathbf{K}$.

4.4. Effectiveness of the VTCR

The capabilities of the method have been demonstrated on complex assemblies of plates [20, 21, 22]. Comparisons with industrial finite element codes showed that the VTCR is capable of predicting

the effective quantities at a very low cost. The method was also extended to shells in [23] and heterogeneities were included in [24].

4.5. The wide-frequency-range analysis

In our proposed approach to the transient dynamic response analysis, the Frequency Response Function (FRF) over a very wide frequency range needs to be calculated. Therefore, the ability to use the VTCR over a relatively wide frequency range could be advantageous.

4.5.1. Calculation of the VTCR in a frequency range Thus, the objective is to be able to calculate the solution in a frequency range B with central frequency ω_0 and bandwidth $2\Delta\omega$: Find $\underline{U}$ which verifies:

$$\mathbf{K}^h(\omega)\underline{U}(\omega) = \underline{F}^h(\omega) \qquad \forall \omega \in B = [\omega_0 - \Delta\omega; \omega_0 + \Delta\omega] \tag{24}$$

The idea is to introduce a two-scale approximation in terms of ω. Any quantity α, including the operator $\mathbf{K}^h(\omega)$ and the load $\underline{F}^h(\omega)$, can be written over $\omega \in B$ as:

$$\alpha(\omega) = \sum_{r=1}^{l} Q_r(\omega) A_r(\omega_0) \tag{25}$$

where A_r is assumed to be constant over B. If necessary, one could build a better approximation for function A_r, e.g. a linear approximation. Q_r is a rapidly varying function of ω equal to:

$$Q_r(\omega) = \mathrm{e}^{2\pi i \omega q_r}$$

where q_r is one of the discrete values: $\{r\xi | r = -N, -N+1, \ldots, 0, 1, 2, \ldots, N\}$.
In practice, $2\omega_c N\xi$ is equal to the maximum number of space waves per substructure. ξ or N is a parameter which characterizes the quality of the two-scale approximation (25) ($N \sim 100$ to 1000). Several techniques have been developed for determining an approximation of $\underline{U}$ in the form of (25) [25]. Here, we will introduce a new and quite efficient version.

Let us study the behavior of the exponential argument. This quantity can be expanded into a Taylor series up to order $\bar{k}$. The matrix $\mathbf{K}^h$ and load vector $\underline{F}^h$ can then be approximated as:

$$\mathbf{K}^h(\omega) = \sum_{k=0}^{\bar{k}} \mathbf{K}_k(\omega_0)(\omega - \omega_0)^k \tag{26}$$
$$\underline{F}^h(\omega) = \sum_{k=0}^{\bar{k}} \underline{F}_k(\omega_0)(\omega - \omega_0)^k$$

Let us also define the mean value over the frequency range B:

$$\langle \cdot \rangle = \frac{1}{2\Delta\omega} \int_B \cdot \, \mathrm{d}\omega$$

The matrix $\mathbf{K}^h$ and load vector $\underline{F}^h$ can be expressed as:

$$\mathbf{K}^h(\omega) = \langle \mathbf{K}^h \rangle + \Delta\mathbf{K}(\omega) \tag{27}$$
$$\underline{F}^h(\omega) = \langle \underline{F}^h \rangle + \Delta\underline{F}(\omega)$$

According to the Taylor expansion (26), one has:

$$\Delta\mathbf{K}^h(\omega) = \sum_{k=0}^{\bar{k}} \Delta\mathbf{K}_k(\omega_0)(\omega-\omega_0)^k \tag{28}$$

$$\Delta\underline{F}^h(\omega) = \sum_{k=0}^{\bar{k}} \Delta\underline{F}_k(\omega_0)(\omega-\omega_0)^k$$

$\underline{U}$ can also be defined using the same approach:

$$\underline{U}^h(\omega) = \langle\underline{U}^h\rangle + \Delta\underline{U}(\omega) \tag{29}$$

Over the frequency range B, Equations (24), (27) and (29) can be rewritten as:

$$\left[\langle\mathbf{K}^h\rangle + \Delta\mathbf{K}\right]\left[\langle\underline{U}\rangle + \Delta\underline{U}\right] = \langle\underline{F}^h\rangle + \Delta\underline{F} \tag{30}$$

Equation (30) involves terms of very different magnitudes: some are large while others are small. Using the techniques of perturbation methods, different order terms can be identified and Equation (30) can be rewritten for order 0 and order 1:

$$\begin{aligned} &\langle\mathbf{K}^h\rangle\langle\underline{U}\rangle = \langle\underline{F}^h\rangle && \text{order 0} \\ &\langle\mathbf{K}^h\rangle\Delta\underline{U} = -\Delta\mathbf{K}\langle\underline{U}\rangle + \Delta\underline{F} && \text{order 1} \end{aligned} \tag{31}$$

with $\Delta\underline{U}$ equal to:

$$\Delta\underline{U} = \sum_{k=0}^{\bar{k}} \Delta\underline{U}_k(\omega_0)(\omega-\omega_0)^k \tag{32}$$

Finally, the displacement retained over the frequency range B is:

$$\underline{U} = \lambda\langle\underline{U}\rangle + \mu\Delta\underline{U} \tag{33}$$

where λ and μ minimize the error defined through the approximations in (31):

$$E^2 = \frac{1}{2\Delta\omega}\int_B \left[\underline{F}^h - \mathbf{K}^h\underline{U}\right]^T \left[\mathbf{K}_s^h\right]_D^{-1} \left[\underline{F}^h - \mathbf{K}^h\underline{U}\right] \mathrm{d}\omega \tag{34}$$

$\left[\mathbf{K}_s^h\right]_D$ is the diagonal of the symmetric part of $\mathbf{K}^h$, which is a slowly-varying function.

Remarks:

- $\bar{k}$ corresponds to the degree of the Taylor expansion and is the only parameter that must be chosen to ensure good accuracy.
- The mean dissipated energy is:

$$e = \frac{\lambda^2}{2}\langle\underline{U}\rangle^T\mathbf{K}_s^h\langle\underline{U}\rangle + \frac{\mu^2}{4\Delta\omega}\int_B \Delta\underline{U}^T\mathbf{K}_s^h\Delta\underline{U}\,\mathrm{d}\omega \tag{35}$$

- λ, μ can be ω-functions.

This method over a frequency range was tested on beams and on assemblies of plates in [26]. For $\frac{\Delta\omega}{\omega_0} \approx 10\%$, $\bar{k} = 5$ seems to yield a very good approximation.

4.5.2. Use of the wide-frequency-range analysis In the frequency-domain analysis procedure, the use of discrete Fourier transforms requires that the forcing functions $\underline{f}_d(t)$ and $\underline{F}_d(t)$ in the dynamic reference problem of Equation (4) be converted into periodic forms. Thus, unless the forcing functions $\underline{f}_d(t)$ and $\underline{F}_d(t)$ and the unit impulse function of the system $\underline{h}(t)$ are time-limited and the time period T_o is selected carefully, the initial conditions of the transient response of the structure may not be satisfied. This situation would arise because of an overlap with previous periods of the time function, as explained in [27].
Therefore, the observation time T_o must be chosen such that the transient response of the damped system dies out by the end of T_o. The choice of T_o is directly reflected in the frequency sampling of the frequency response function $\underline{\hat{h}}(\omega)$ and can lead to a large number of VTCR calculations. It is, therefore, crucial to be able to know the frequency response function for any frequency in a relatively wide frequency range, as we did in Section 4.5.1: then, the frequency step can be chosen anyhow with no increase in computation effort.

Then, since the FRF is known explicitly over a wide frequency range, the frequency-domain analysis using discrete Fourier transforms can be carried out easily.

5. EFFECTIVENESS OF THE METHOD

5.1. Example of a beam subjected to a shock at one end

Figure 5 shows an example consisting of two beams connected together, subjected to an impact bending load at the right end and fixed at the left end.

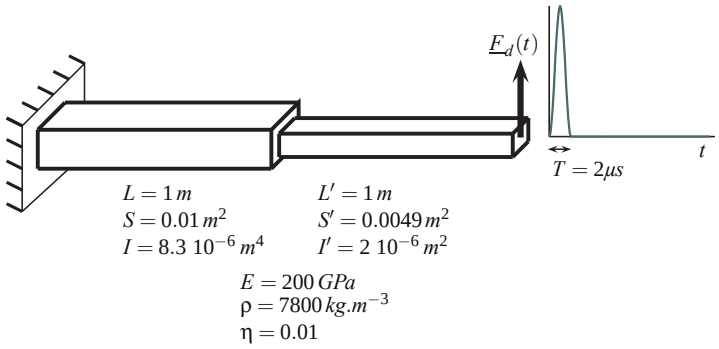

Figure 5. A transient dynamic problem: beam subjected to impact bending

The loading which characterizes the impact and its spectrum obtained through the Fourier transform are described in Figure 6.
We chose the observation time T_o such that the transient response of the damped system dies out by the end of this lapse of time: this enabled us to use discrete Fourier transforms.

The purpose of this example is to show the importance of the medium frequencies which, although the displacements are small, can play a significant role in the the kinetic energy. We will also use this example to compare our approach with a classical finite element method in the time domain.

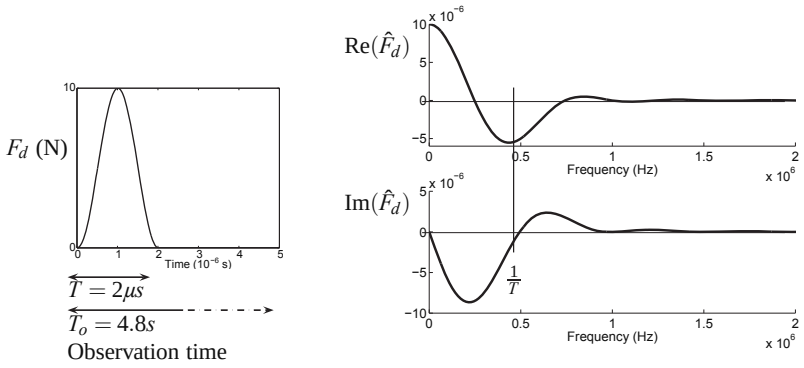

Figure 6. The loading and its spectrum

5.2. The discretized problem of the frequency-domain approach

The frequency range $[0, \omega_c']$ being studied was divided into two parts: the low frequencies $[0, \omega_c]$ and the medium frequencies $[\omega_c, \omega_c']$.

As suggested in Section 3.2, a standard finite element technique was used to obtain the frequency response functions over the low-frequency range. In order to derive a proper FRF, the reduced basis was constructed from the first m modes to arrive at a highest eigenfrequency $\omega_m = 2\omega_c$, and was completed with the static bending mode. The mesh was discretized according to the classic law "at least 7 elements per wavelength" for the highest eigenmode of the reduced basis.
The VTCR turned out to be a suitable computational method for the medium-frequency range and used only eight complex rays: two interior ones and two evanescent ones for each beam.

The problem to be solved was a discrete frequency problem, since the spectrum of the loading was obtained via the efficient Fast Fourier Transform [27]. Thus, the FRF was calculated for every sampling frequency. The sampling was a function of the observation time T_o of the response : $f_o = \frac{1}{T_o}$.
The number of VTCR calculations for the medium-frequency range was reduced by using the wide-frequency-range analysis of the VTCR presented in Section 4.5, which was essential in that case. Degree $k = 5$ of the Taylor expansion was chosen.

Having calculated the FRF, we performed an inverse Fast Fourier Transform in order to restore the time-dependent response, which led to no difficulty thanks to the wide-range analysis of the VTCR (see Section 4.5.2).

5.3. Choice of the frequency ranges

The frequency range $[0, \omega_c']$ being studied was divided into two parts: the low frequencies $[0, \omega_c]$ and the medium frequencies $[\omega_c, \omega_c']$. We will now study the influence of these ranges.

5.3.1. Influence of ω_c Let us vary ω_c first. Figure 7 shows the velocities at the junction of the two beams obtained with three different values of ω_c and a fixed value of $\omega_c' = 10^6 Hz$. On the left-hand side, the velocity is represented over a rather large time span; the right-hand side of Figure 7 is a zoom on the beginning of that signal. The different values of ω_c are chosen such that $\omega_c = [16\,10^3 Hz, 65\,10^3 Hz, 145\,10^3 Hz]$ generate maxima of 5, 10 and 20 oscillations respectively on one of the two beams.

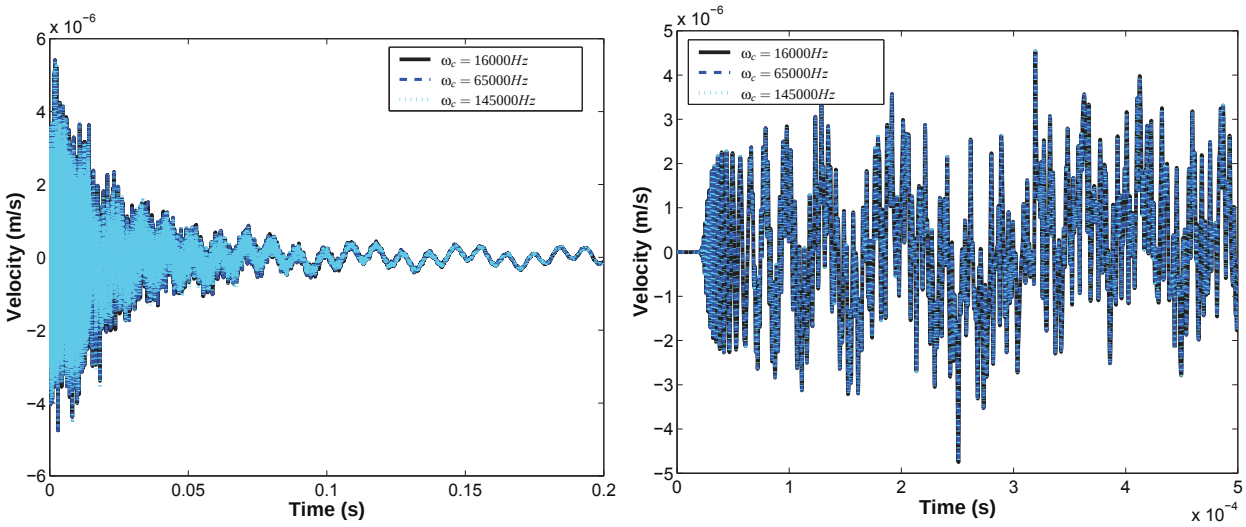

Figure 7. Deflection at the junction for different values of ω_c

As expected, the choice of ω_c does not affect the accuracy of the response. Indeed, the frequency contents of the three responses are the same; only the ways the frequency response function over part of the frequency range are obtained are different, but in each case the FRF is calculated over the same global frequency range.
Nevertheless, the choice of ω_c affects the cost of the calculation: a large ω_c would require an expensive reduced basis in order to calculate the FRF over $[0,\omega_c]$ (see Section 3.2). This could also lead to numerical difficulties.
In practice, ω_c is chosen such that this frequency does not generate more than 10 oscillations per beam. Beyond 10 oscillations, the frequency is considered to belong to the medium-frequency domain. In the example presented, we had $\omega_c = 65000Hz$.

5.3.2. Influence of ω_c' Figure 8 shows the influence of ω_c', i.e. the effect of the frequency content on the response. On the left-hand side, the velocity is represented over a rather large time span; the right-hand side of Figure 7 is a zoom on the beginning of that signal. The velocities at the junction of the two beams obtained with three different values of ω_c' and a fixed value of $\omega_c = 65000Hz$ are shown. The values of ω_c' were chosen as follows: $\omega_c' = [\frac{1}{2T}, \frac{1}{T}, \frac{2}{T}] = [0.25\,10^6 Hz, 0.5\,10^6 Hz, 10^6 Hz]$, T being the length of the impact (Figure 6).

One can observe that the frequency content of the response affects the velocity and, therefore, the kinetic energy to a great extent. In order to evaluate the frequency range necessary to derive the correct response, the maximum of the kinetic energy at the junction of the two beams during the observation time is plotted on Figure 9 as a function of the frequency range taken into account in the response.

In this case, the frequency range which is necessary and sufficient to produce the correct energy level seems to be $[0, 10^6 Hz]$; this range is designated on Figure 9 by the vertical solid line. $\omega_c' = 10^6 Hz$ is twice the characteristic frequency $\frac{1}{T}$ of the input signal. From here on, ω_c' will be chosen such that: $\omega_c' = \frac{2}{T} = 10^6 Hz$. Looking at the spectrum of the impact loading in Figure 6, this criterion $\omega_c' = \frac{2}{T}$ enables one to embrace most of the frequency content of the input signal.
In the above example, $\omega_c' = 10^6 Hz$ corresponds to an excitation generating 40 oscillations per beam.

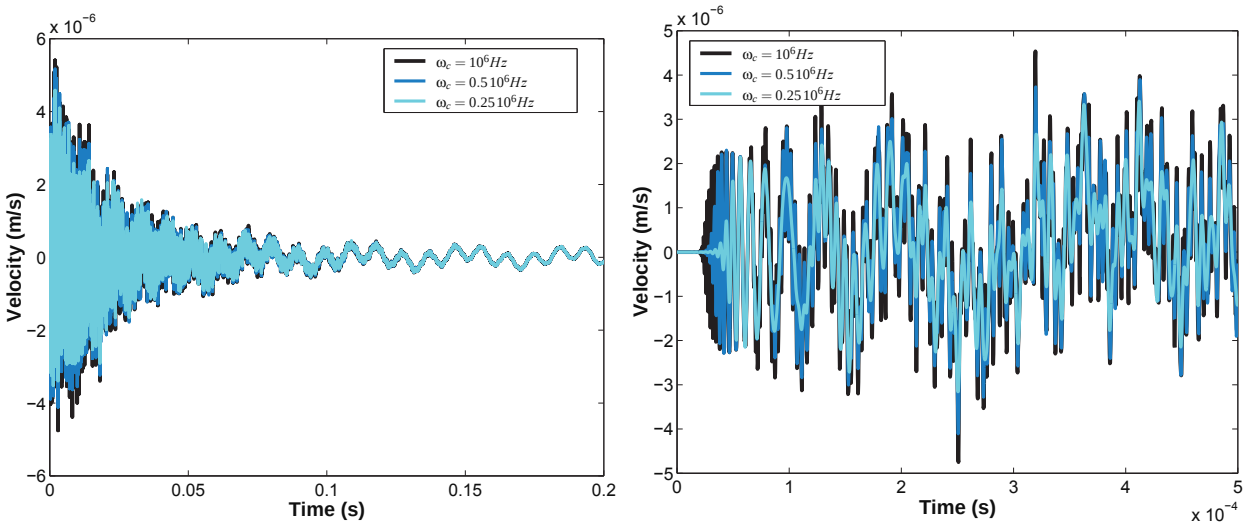

Figure 8. Deflection at the junction for different values of ω_c'

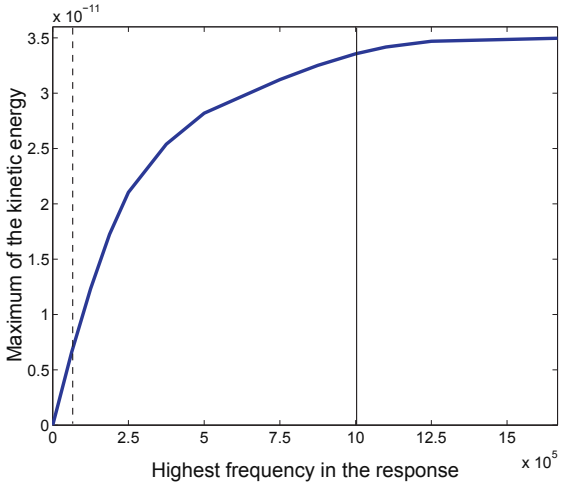

Figure 9. Maximum of the kinetic energy at the junction of the two beams during the observation time as a function of the frequency range taken into account

5.3.3. Summary of the frequency ranges chosen The different frequency ranges are described in Figures 9 and 10: the vertical dashed lines represent the limit of the low-frequency range and the vertical solid lines show the upper bound of the medium-frequency range, i.e. the frequency content of the response. These frequency ranges will be used from here on for the remaining examples.

Table I summarizes the content of each frequency range.

The number of VTCR calculations for the medium-frequency range was reduced from $4,800,000$ to $1,000$ only by using the wide-frequency-range analysis of the VTCR presented in Section 4.5, which was essential in this case.

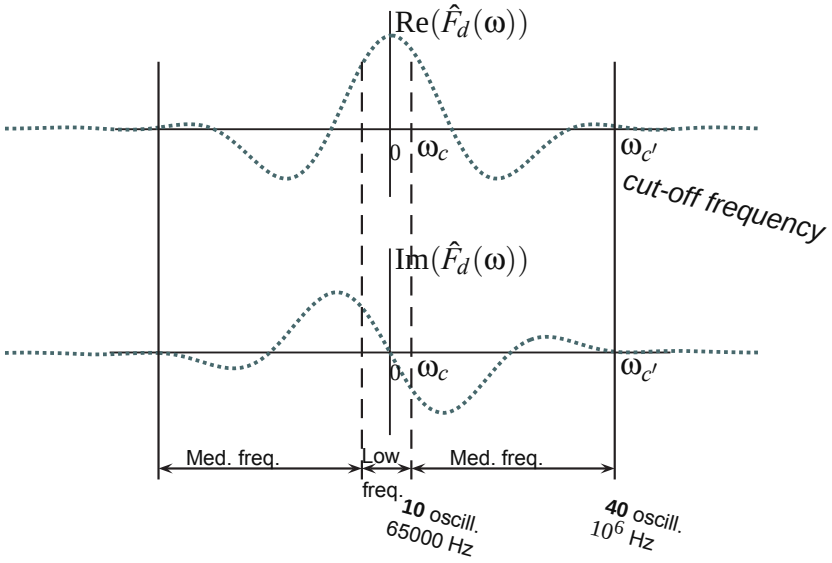

Figure 10. Frequency spectrum of the loading and the different frequency ranges

Table I. Content of each frequency range

Frequency range	Low	Medium
Method	Reduced basis: 53 modes	VTCR: 8 rays
Frequency range	$[0, 65,000Hz]$	$[65,000Hz, 10^6Hz]$
Nb. of sampling frequencies	$308,600$	$4,800,000$
		$\Rightarrow \mathbf{1,000}$ calculations

5.4. Importance of the medium frequencies

The importance of the medium frequencies has already been pointed out in Section 5.3.2. Figure 9 shows that taking into account the low frequencies alone (vertical dashed line) alters the kinetic energy level.
Further comparisons emphasizing the importance of the medium frequencies can be made on the same example. Let us consider two responses obtained with the frequency-domain approach, one taking the medium-frequency range into account and the other ignoring it.

The deflections at the junction of the two beams with and without the medium-frequency content are plotted in Figure 11.

On the left-hand side of Figure 11, the responses seem to be similar, but when zooming in on the very beginning of the signal (on the right-hand side), one notices differences: in the absence of the medium frequencies, the small oscillations due to these frequencies are killed.
Although the displacements due to the medium frequencies are small, the velocity and, therefore, the kinetic energy due to these oscillations are very significant (Figure 12).

This velocity and this kinetic energy are even larger if one uses a damping law which decreases with

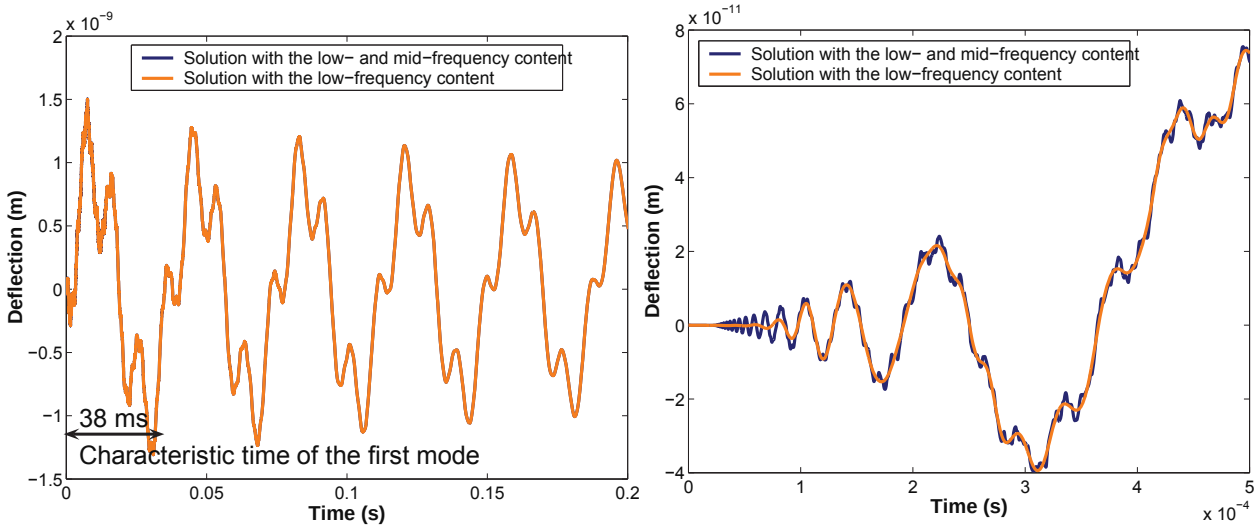

Figure 11. Deflection at the junction

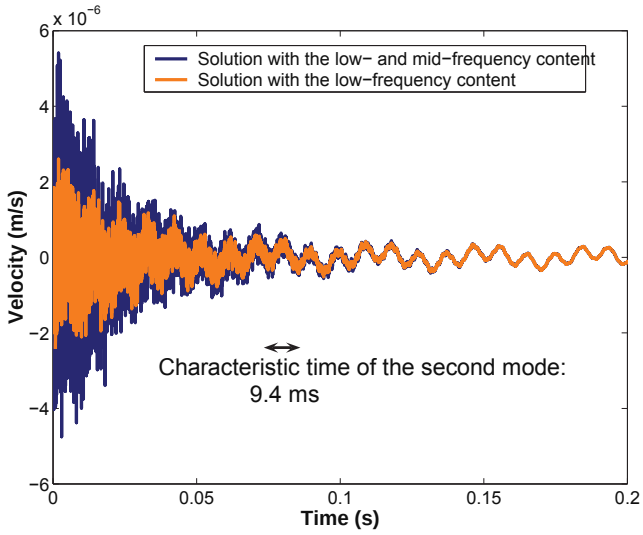

Figure 12. Velocity at the junction

the frequency, as shown in Figure 13. Damping was taken as follows:

$$\omega \in [0, \omega_0] \qquad \eta = 0.01$$

$$\omega \geq \omega_0 \qquad \eta = 0.01 \left(\frac{\omega_0}{\omega}\right)^{\alpha}$$

with $\omega_0 = 1,000 Hz$. The maximum of the kinetic energy at the junction of the two beams during the observation time is plotted in Figure 13 as a function of α.

The more rapidly the damping decreases with the frequencies, the higher the kinetic energy level when the medium frequencies are taken into account (black line). If one leaves out these frequencies in the response, most of the kinetic energy is ignored (grey line), especially for high values of α.

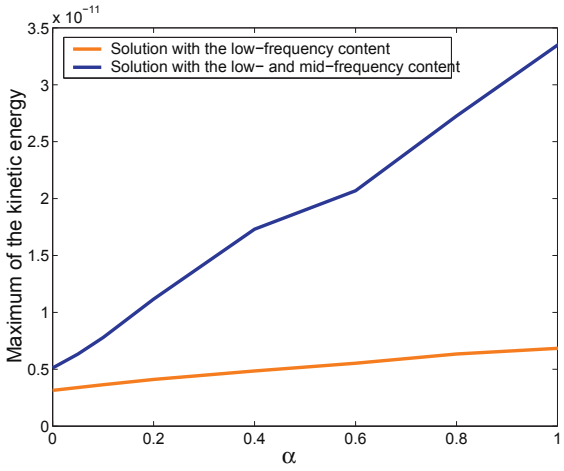

Figure 13. Maximum of the kinetic energy at the junction of the two beams during the observation time as a function of α

This example emphasizes the importance of the medium-frequency range. Therefore, one cannot leave out the medium frequencies, as these appear to a great extent in the velocity and, consequently, in the kinetic energy. Ignoring these medium frequencies could lead to poor design of structures.

5.5. Comparison with a standard approach

Let us now compare the response obtained with our frequency-domain approach with that obtained with a standard time-domain approach. The purpose of this comparison is to assess the effectiveness of the new method.

The calculation of the response with the time-domain approach was carried out in such a way that it produced the same high-frequency content as our frequency approach, i.e. 40 oscillations per beam for the highest frequency taken into account. To achieve that result, the finite element model required a fine mesh with 280 finite elements per beam, i.e 7 elements per oscillation. Classically, an explicit time scheme with a time step based on the Courant-Friedrichs-Levy condition for the highest frequency was used. Since the spatial discretization was very dense in order to take into account the medium frequencies, this means that the time-domain method required a very large number of time steps. Indeed $320,000$ time steps per time period of the first eigenmode of the structure were necessary. The integration of the time scheme could be achieved using the reduced basis with 146 modes.

Table II summarizes the sizes of the computational problems for the two methods: the frequency-domain approach proposed in this paper and the classical time-domain approach. The period of time of interest T_1 is the time period of the first eigenmode of the structure.

The two responses are plotted in Figures 14 and 15. These show respectively the deflection and the velocity at the junction of the two beams obtained with the time-domain approach (dashed lines) and the new frequency-domain approach (solid lines).

On the left-hand side of Figures 14 and 15, the responses obtained with both approaches are very similar, even when one zooms in on the very beginning of the signal (on the right-hand side).
If one takes the response obtained with the classical time-domain approach as the reference, the conclusion from this comparison is that our method yields good results containing a wide frequency content.

Table II. Sizes of the computational problems for the time-domain (TD) and the frequency-domain (FD) approaches (period of time of interest: $T_1 = 38ms$)

Approach	TD	FD	
	Reduced basis	Reduced basis	VTCR
Finite elements (beams)	276	98	
Eigenmodes	146	53	
Complex rays			8
Number of calculations	$320,000$	$308,600$	1,000
Size of the computational problem	$320,000 \times 146$	$308,600 \times 53 + 1,000 \times 8$	

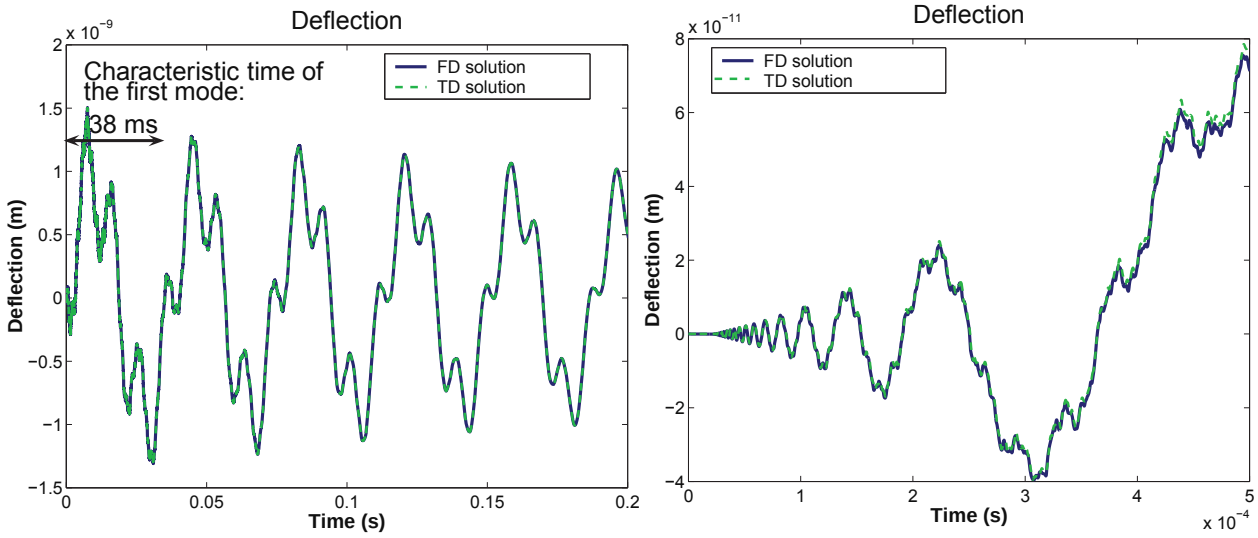

Figure 14. Deflections at the junction

Furthermore, the results of the new method were obtained with a reduced numerical effort. Indeed, the calculations for our approach were carried out in the low-frequency range using a small reduced basis compared to that of the time-domain approach (see Table II). For more complex structures, in the time-domain approach, the construction of a reduced basis sufficiently rich in modes to deal with fast dynamics, such as shocks, is often unfeasible; therefore, in these cases, the time integration is carried out on the finite element matrices directly: this leads to even greater computation times. In our method, thanks to the use of the wide-frequency-range analysis of the VTCR, the frequency content is extended using only 1,000 VTCR calculations. The frequency domain analysis procedure also requires discrete Fourier transforms, which are performed using the Fast Fourier Transform (FFT) algorithms. The use of the FFT makes the frequency approaches efficient for the analysis of the dynamic response of linear systems [28].

The weakness of the frequency-domain approach lies in the fact that regardless of the period of time of interest T_1, the response must be calculated for an observation time T_o long enough for the response of the damped system to die out. This constraint, mentioned in Section 4.5, is due to the discrete Fourier

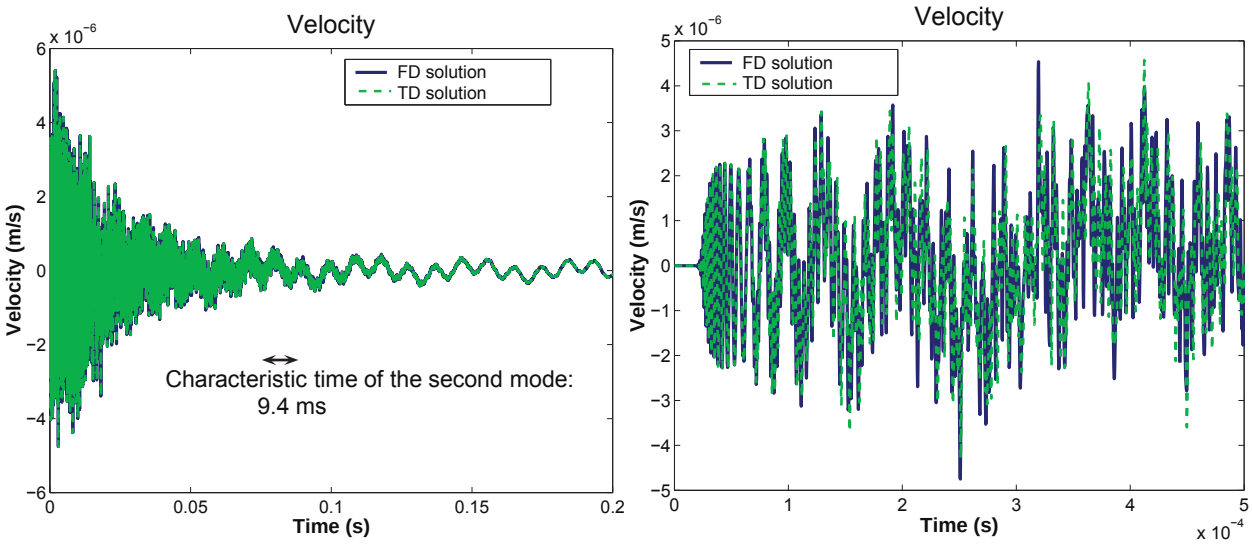

Figure 15. Velocities at the junction

transform and its periodic properties.
Nevertheless, the extension of the observation time requires only a finer sampling of the frequencies, which creates no particular difficulties since the wide-frequency-range analysis of the VTCR is used in our approach; but it still takes memory to store the data.
The following section deals with the means of reducing the number of frequency samples by taking advantage the quick fading-out of the medium frequencies.

5.6. Improvement of the proposed frequency-domain approach

Here, we focus on the properties of the medium frequencies in order to reduce the number of frequency samples for the calculation of the frequency response function over the medium-frequency range. Indeed, since the bending beam being studied is a scattering medium, the propagation velocity of the medium frequencies is greater than that of the low frequencies; therefore, the time taken by the medium frequencies to become negligible (Figure 16) is rather short compared to the observation time $T_0 = 4.5s$ necessary in order to use the Fourier transform techniques.

Therefore, in Equation (36), the time response can be viewed as the superposition of two components, $f_{low}(t)$ and $f_{mid}(t)$, corresponding to the low-frequency contribution $\hat{f}_{low}(\omega)$ and the medium-frequency contribution $\hat{f}_{mid}(\omega)$ respectively.

$$\begin{aligned} f(t)_{t\geq 0} &= \frac{1}{2\pi}\int_{-\infty}^{+\infty} \hat{f}_{low}(\omega)\, \mathrm{e}^{i\omega t}\, \mathrm{d}\omega + \frac{1}{2\pi}\int_{-\infty}^{+\infty} \hat{f}_{mid}(\omega)\, \mathrm{e}^{i\omega t}\, \mathrm{d}\omega \\ &= f_{low}(t) + f_{mid}(t) \end{aligned} \tag{36}$$

These two components can be calculated separately. $f_{low}(t)$ is obtained easily with any suitable and efficient approach; the medium-frequency contribution $f_{mid}(t)$ is obtained with the frequency-domain approach presented in this paper and added afterwards. Calculating the two components separately is convenient because in the calculation of $f_{mid}(t)$ the low frequencies are put aside and the medium frequencies alone are taken into account. Thus, one can take advantage of the rapid fading-out of

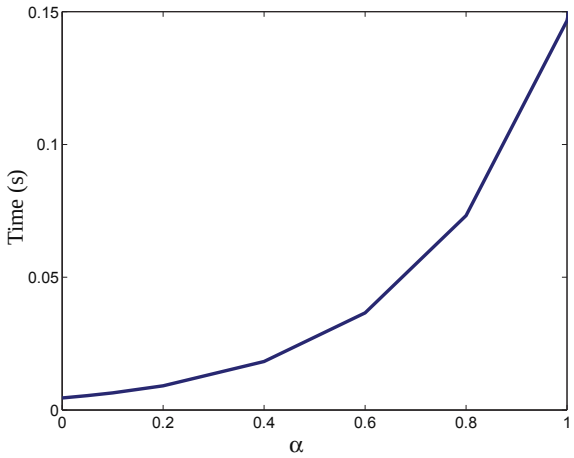

Figure 16. Time taken by the medium frequencies to die out as a function of α

these medium frequencies in the time response to shorten the observation time for the discrete Fourier transform to a considerable extent, which reduces the frequency sampling of the FRF $\hat{f}_{mid}$ over the medium-frequency range.

The velocities and the maxima of the kinetic energy as functions of α are compared in Figures 17 and 18: one response was obtained with the FD approach presented in the previous sections and the other with the technique of superposition of the low- and mid-frequency components we just described.

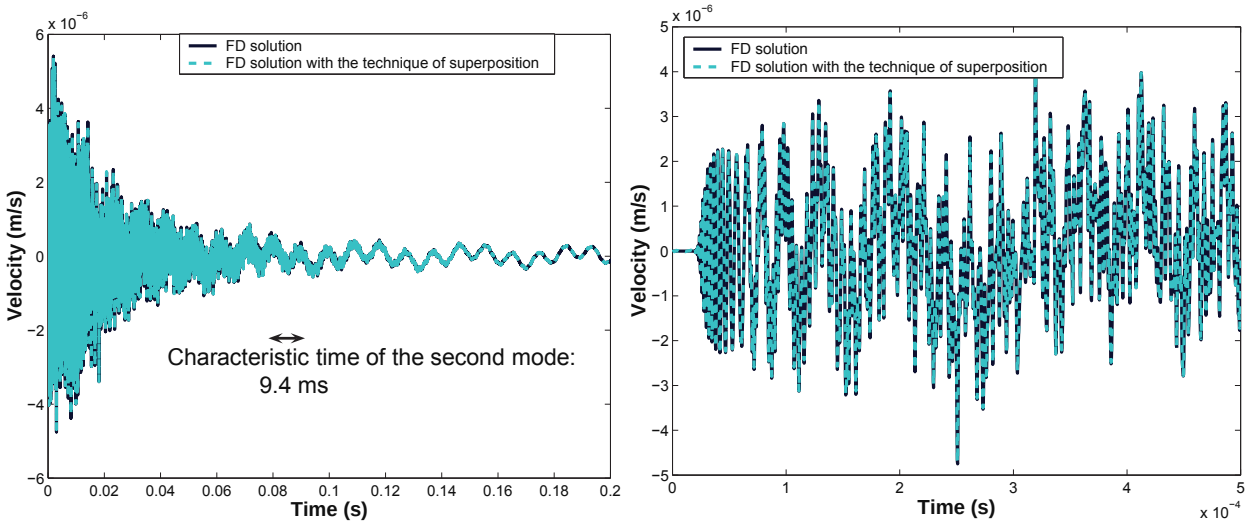

Figure 17. Velocity at the junction

The superposition of the two components yields very good results and requires far fewer frequency samples for the calculation of the frequency response function over the medium-frequency range. The fraction $\frac{N_s}{N}$ of the frequency samples for which the FRF $\hat{f}_{mid}$ had to be calculated over the medium-frequency range is shown in Figure 19: N_s and N are the numbers of frequency samples over the medium-frequency range needed for the frequency-domain approach, with and without the

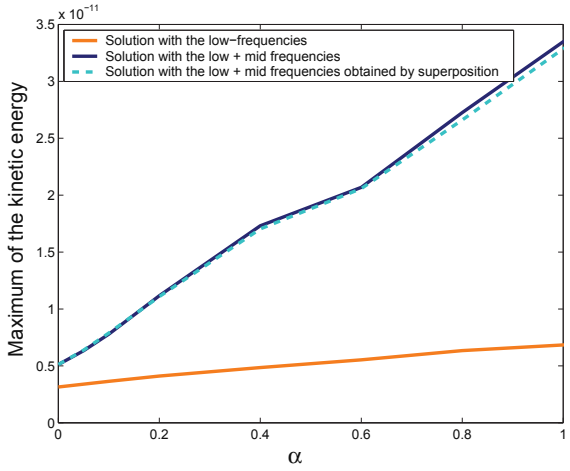

Figure 18. Maximum of the kinetic energy at the junction of the two beams during the observation time as a function of α

superposition technique respectively.

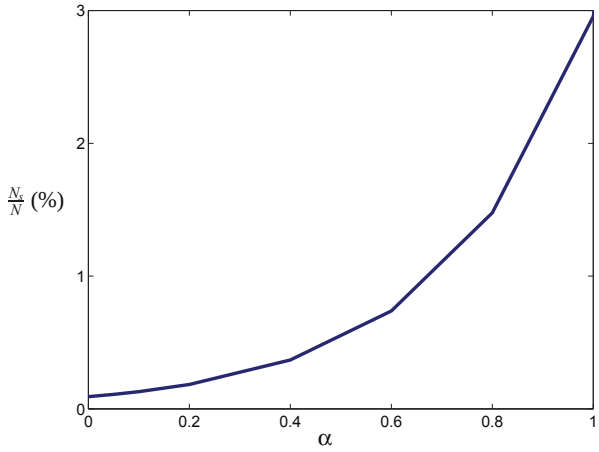

Figure 19. Comparison of the numbers of frequency samples

The number of frequency samples over the medium-frequency range for which the FRF $\hat{f}_{mid}$ needs to be calculated for the frequency-domain approach is considerably smaller when the components arising from the medium-frequency and from the low-frequency contributions are calculated separately.

6. CONCLUSION

A new theory for the calculation of transient dynamic responses with a high frequency content, has been introduced and its effectiveness has been shown. The point of this technique is to cover both the low and the medium frequencies, while decreasing the cpu-time. In this paper, only non-linearities in the frequency domain have been considered. The extension to non-linearities expressed in the time

domain and to 3D-problems is the subject of further developements.

REFERENCES

1. Bathe KJ. *Finite Element Procedures* (2nd edn). Prentice Hall, 1996.
2. Belytschko T, Liu W, Moran B. *Nonlinear Finite Elements for Continua and Structures*. John Wiley & Sons, 2000.
3. Lyon RH, Maidanik G. Power flow between linearly coupled oscillators. *Journal of the Acoustical Society of America* 1962; **34**(5):623–639.
4. Ilhenburg F, Babuška I. Dispersion analysis and error estimation of Galerkin finite element methods for Helmholtz equation. *International Journal for Numerical Methods in Engineering* 1995; **38**:3745–3774.
5. Deraemaeker A, Babuška I, Bouillard P. Dispersion and pollution of the fem solution for the Helmholtz equation in one, two and three dimensions. *International Journal for Numerical Methods in Engineering* 1999; **46**:471–499.
6. Farhat C, Harari I, Hetmaniuk U. A discontinuous Galerkin method with Lagrange multipliers for the solution of Helmholtz problems in the mid-frequency regime. *Computer Methods in Applied Mechanics and Engineering* 2003; **192**:1389–1419.
7. Harari I, Haham S. Improved finite element method for elastic waves. *Computer Methods in Applied Mechanics and Engineering* 1998; **166**:143–164.
8. Liu WK, Zhang Y, Ramirez MR. Multiple scale finite element methods. *International Journal for Numerical Methods in Engineering* 1991; **32**:969–990.
9. Morand JPH. A modal hybridization method for the reduction of dynamic models. In *New Advances in Computational Structural Mechanics*, Ladevèze P, Zienkiewicz O (eds). Elsevier, 1992; 347–365.
10. Soize C. Reduced models in the medium frequency range for general dissipative structural-dynamics systems. *European Journal of Mechanics* A/Solids 1998; **17**(4):657–685.
11. Sarka A, Ghanem R. Mid-frequency structural dynamics with parameter uncertainty. *Computer Methods in Applied Mechanics and Engineering* 2002; **191**:5499–5513.
12. Desmet D, Van Hal B, Sas P, Vandepitte D. A computationally efficient prediction technique for the steady-state dynamic analysis of coupled vibro-acoustic systems. *Advances in Engineering Software* 2002; **33**:527–540.
13. Belov VD, Ryback SA. Applicability of the transport equation in the one-dimensional wave propagation problem. *Journal of Soviet Physics-Acoustics* 1975; **21**(2):110–114.
14. Ichchou MN, Le Bot A, Jézéquel L. Energy model of one-dimensional, multipropagative systems. *Journal of Sound and Vibration* 1995; **201**(5):535–554.
15. Langley RS. On the vibrational conductivity approach to high frequency dynamics for two-dimensional structural components. *Journal of Sound and Vibration* 1995; **182**(4):637–657.
16. Lase Y, Ichchou MN, Jézéquel L. Energy flow analysis of bars and beams: theoretical formulation. *Journal of Sound and Vibration* 1994; **192**(1):2981–3005.
17. Ladevèze P. A new computational approach for structure vibrations in the medium frequency range. *Compte rendu de l'académie des sciences de Paris*, Sér. II, 1996; **322**(12):849–856.
18. Ladevèze P. A new computational method for medium-frequency vibrations and its extension to transient dynamics. In *Proceedings of the Seventh International Conference on Computational Plasticity*, Owen DRJ, Oñate E, Suárez B (eds). CIMNE: Barcelona, 2003.
19. Deraemaeker A, Ladevèze P, Leconte P. Reduced basis for model updating in structural dynamics based on constitutive relation error. *Computer Methods in Applied Mechanics and Engineering* 2002; **191**:2427–2444.
20. Ladevèze P, Arnaud L. A new computational method for structural vibrations in the medium frequency range. *Computer Assisted Mechanics and Engineering Sciences* 2000; **7**:219–226.
21. Ladevèze P, Arnaud L, Rouch P, Blanzé C. The variational theory of complex rays for the calculation of medium-frequency vibrations. *Engineering Computations* 2001; **18**(1):193–214.
22. Rouch P, Ladevèze P. The variational theory of complex rays: a predictive tool for medium-frequency vibrations. *Computer Methods in Applied Mechanics and Engineering* 2003; **192**:3301–3315.
23. Riou H, Ladevèze P, Rouch P. Extension of the variational theory of complex rays to shells for medium-frequency vibrations. *Journal of Sound and Vibration* 2004; **272**:341–360.
24. Ladevèze P, Blanc L, Rouch P, Blanzé C. A multiscale computational method for medium-frequency vibrations of assemblies of heterogeneous plates. *Computers and Structures* 2003; **81**(12):1267–1276.
25. Ladevèze P, Rouch P, Riou H, Bohineust X. Analysis of medium-frequency vibrations in a frequency range. *Journal of Computational Acoustics* 2003; **11**(2):255–283.
26. Ladevèze P, Riou H. Computation of medium-frequency vibrations over a large frequency range. *Computer Methods in Applied Mechanics and Engineering* Submitted.
27. Brigham EO. *The Fast Fourier Transform and its Applications*. Prentice-Hall: Englewood Cliffs, 1988.
28. Clough RW, Penzien J. *Dynamics of Structures* (2nd edn). McGraw-Hill Education, 1993.